# Comparing zonal and CFD models of air flows in large indoor spaces to experimental data.

**Laurent Mora** [†], **Ashok Gadgil**[*] **and Etienne Wurtz**[†]

[*] Lawrence Berkeley National Laboratory, Berkeley, CA 94720, USA

[†] L.E.P.T.A.-B., University of La Rochelle, 17042 La Rochelle, France

## Abstract

Algebraic multi-zone infiltration models (e.g. COMIS, CONTAM) have been developed to predict air flows and contaminant transport in complex buildings. However these models assume that each building zone is a well-mixed volume. This assumption is not appropriate to model large indoor spaces. We describe two simplified approaches, called zonal methods, to describe air flows in large indoor spaces, intended to provide an improvement over the well-mixed assumption.

We compare velocity predictions from different formulations of zonal methods and coarse-grid $k-\epsilon$ CFD models, to measurements, in a 2D mechanically-ventilated isothermal room. Our results suggest that coarse-grid CFD is a better simplified method to predict air flows in large indoor spaces coupled to complex multizone buildings, than are the zonal methods when airflow details are required. Based on the comparison of pressure predictions from the different models, we propose a way of coupling a model of detailed airflow in large spaces to an algebraic multi-zone infiltration model.

**Key words** Indoor air; CFD; zonal; air flow; simulation.

## Nomenclature

- $a$ velocity profile parameter ($a = 1/7$)
- $C$ empirical 'permeability' coefficient [$\mathrm{m \cdot s^{-1} \cdot Pa^{-n}}$]
- $g$ gravitation acceleration [$\mathrm{m \cdot s^{-2}}$]
- $k_s$ coefficient defined uniquely for each cell position with $k_s \approx 4/(4n_s - 3)$ for central cells of odd meshes or $k_s \approx 2/(2n_s - 1)$ for all other cells
- $n$ power-law coefficient usually taken as $n = 0.5$ for turbulent flows
- $n_s$ cell position index $n_s = 1, 2, 3, \ldots$ relative to the nearest wall surface
- $P_i$ pressure in cell $i$ at the altitude $z_i$ [Pa]
- $S$ surface area shared between cells $i$ and $j$ [$\mathrm{m^2}$]
- $w$ width of cells $i$ and $j$ [m]
- $z_i$ altitude of the center of the cell $i$ [m]

*Greek symbols*

- $\Delta z$ height of cells $i$ and $j$ [m]
- $\kappa$ universal constant with an empirically determined value ranging from 0.36 to 0.40
- $\rho$ average density of air in the two adjacent cells [$\mathrm{kg \cdot m^{-3}}$]
- $\tau_{zr}$ time-smoothed shear stress

## 1 Introduction

Indoor environment design requires detailed informations about air distribution, such as airflow pattern, velocity, temperature, humidity, and pollutant concentrations. Because experimental measurement cannot be a practical design tool, various numerical methods have been developed to simulate the indoor environment. A popular approach of computational simulations is the Computational Fluid Dynamics (CFD) method. However, solving commonly used turbulence models requires fast computers with large amount of memory. So this approach has mostly been limited to study details of air distribution in single rooms.

Multi-zone infiltration and airflow models such as COMIS [1] and CONTAM [2] have been developed to predict air flows in complex buildings. These models are suitable tools to design ventilation systems for complex buildings, as well as to provide necessary inputs for energy analysis tools. They can predict air flows and contaminant transport within the entire building, but based on a strong assumption. This building is defined as a set of well-mixed volumes or *zones* of homogeneous com-

position. While this assumption can be acceptable for small rooms or zones, it becomes unacceptable when modeling large indoor spaces such as atria and auditoria.

The present work is part of a research effort aimed at integrating a detailed model of airflow in large spaces with an algebraic multi-zone infiltration model to describe pollutant transport and coupled air flows within and between complex buildings and large spaces. In the past 15 years, zonal models ([3]-[8]) were developed with the goal to obtain an approximate but quicker answer than with CFD models to predict airflow characteristics in large indoor spaces. On the other hand, reducing the number of grids in CFD models is a natural way of decreasing their demand of computational resources to solve air flows in rooms. Therefore, we compare the ability of both zonal and coarse-grid CFD models to predict air flows in a building zone.

In the next section we summarize the requirements imposed by the need to couple a model of large indoor spaces with multi-zone infiltration models. In the third section we briefly describe zonal methods. In the fourth section, we first present airflow patterns predicted using various zonal models and $k-\epsilon$ CFD models, in a mechanically-ventilated isothermal room. Then we present a comparison between velocity predictions from the different formulations of zonal models using the simulation environment SPARK [9], as well as $k-\epsilon$ CFD models, to measurements in the same room provided by Nielsen [10]. And finally we compare the pressure field predictions using the different models. In the last fifth section, we summarize our findings and outline directions for future work.

## 2 Coupling a large space model into a multi-zone infiltration model

Multi-zone infiltration models such as COMIS and CONTAM are based on the assumption that state variables except pressures are homogeneous[1] in each building zone (and the pressure varies hydrostatically). However this assumption is a very poor approximation for the situation in large indoor spaces such as an auditorium or atrium. In order to obtain meaningful predictions of airflow and contaminant dispersion in such spaces, it is necessary to integrate a more detailed model of the space into the multi-zone airflow model.

Multi-zone infiltration models treat each building zone as a single node, and solve the coupled nonlinear algebraic system of equations describing airflows in the whole building, relying on the description of *flow elements* interconnecting the zones. The models treat air as incompressible with temperature-dependent density, and the flow elements, such as cracks or apertures, are described by an algebraic relationship between the mass airflow rate and the difference of pressure accross the element. The pressure variables in such multi-zone infiltration models has the same meaning as in ordinary building science and physics. This meaning (and variable values) must be consistently used in the simplified air flow model of large indoor space, for consistent and successful integrated solution of the coupled problem of airflow in a multi-zone building with a large space.

For example, consider a schematic section of an illustrative 3-story building composed of 3 rooms, one on each floor, connected to an atrium by doorways (see Fig. 1). In this case a multi-zone infiltration model would compute pressure nodes from 1 to 3, while a large space model would be applied to the atrium to calculate pressure nodes 4 through 30. The pressure node 0 is the reference external pressure. The coupling (pressure and air flow) between both models at each doorway location should allow the two models to provide a single self-consistent prediction for the entire building.

## 3 Zonal models

### 3.1 Common practice

Bouia [4] and Wurtz [6] initiated the development of zonal methods based on solving the pressure field to predict airflow and temperatures in large indoor spaces. In the zonal method, the room is subdivided into a number of control volumes or *cells* in which temperature and density are assumed to be homogeneous, while pressure varies hydrostatically. Mass and thermal energy balances are applied to each cell, with air treated as an ideal gas. Airflow between adjacent cells is modeled based on methods used for large openings in ducts. In these methods, the mass flow rate $\dot{m}_{i,j}$ between cell $i$ and cell $j$ is assumed to be governed by a power-law equation as:

$$\dot{m}_{i,j} = C\rho S(\Delta P_{i,j})^n \qquad (1)$$

with $\Delta P_{i,j} = (P_i - \rho_i g z_i) - (P_j - \rho_j g z_j)$. It appears that a value for $C$ of $0.83\,\mathrm{m{\cdot}s^{-1}{\cdot}Pa^{-n}}$ for the whole grid except for the apertures is the consensus among practitioners [11]. Also, the thermal energy flow is determined using a convection-diffusion relationship across the surface between the two cells.

[1] Note that in COMIS different temperatures can be specified within the same zone

This class of models will be called Power-Law models (PL).

Recently, Voeltzel [12] applied this approach to predict airflow patterns and temperature field in atria. For this purpose, she incorporated accurate solutions of radiative exchanges between indoor surfaces and solar gains into a zonal model. For airflow modeling, she used a standard set of power-law flow equations such as equation 1. She obtained good agreement between time-dependent predictions and measurements of temperature. For experiments, she used a 5.1 m-high highly glazed room (ENTPE - SunCell) to validate her zonal model. Temperatures were measured every minute along the vertical centerline of the room at four different heights for 56 hours. Time-dependent temperature predictions demonstrated satisfactory agreement with measurements at these four locations. A zonal model also gave more accurate temperature predictions than a one node model.

In a concurrent and separate research effort, Wurtz et al. [11] pointed out that such classical models cannot adequately represent high velocity regions (e.g. air jets or thermal plumes), owing to the inadequate representation of momentum conservation (by approximating it with a relation between mass flow rate and difference of pressure developed for flows across apertures).

Inard [3] developed an innovative approach to address the inability of the standard zonal method to adequately represent jets and plumes. In order to study the coupling between the thermal plume from a radiator and the airflow in the rest of the room, he patched on to the room model a region for the plume, in which airflow and temperature were defined using known functional relations from textbook idealizations of wall thermal plumes. He, his colleagues, and others extended his method to incorporate free jets, wall jets, and boundary layers in the airflow within the room. Of course, the modeler is presumed to know which specific driven flow idealization to incorporate into the model in each spatial region. This class of zonal models will be identified in this paper as Power-Law models with Specific Driven Flows, or PL-SDF models. In the PL-SDF class of models, Bouia developed an integrated tool (SAMIRA [13]), while Wurtz [6] and Musy [14] developed a library of models within the object-oriented simulation environment SPARK. Wurtz's description allows bidirectional flows across common surfaces shared by cells, while Musy developed an automatic generator of zonal models for complex multi-zone buildings, and integrated new libraries into the zonal model for modeling pollutant transport in the room air, radiative exchange between room surfaces, as well as integrating a finite difference model of conduction heat transfer model through the building envelope.

Inard et al. [15] presented results (performed with SAMIRA) demonstrating good agreement between experimental data and predictions of temperature fields under natural and mixed convection using PL-SDF models. The natural steady-state convection experiment is a 3.1 m×3.1 m×2.5 m cell (CETHIL-MINIBAT test cell), where five wall surfaces are maintained at constant temperature and the sixth surface is in contact with a climatic chamber, allowing control of its surface temperature from -10 to +40 °C. Temperature measurements were collected in 200 locations, with 50 sensors in the central vertical plane. Isotherms predicted by zonal models present a good agreement with isotherms constructed from interpolating measured data in this central plane of the cell. Three steady-state mixed convection cases were investigated (electric heater, hot water radiator, and hot water floor heater) in a ventilated room. Temperature predictions were compared with measurements at 7 different heights along a vertical line in the central plane of the room. This study presents good agreement with experimental data, and highlights the necessity of using an idealized flow model to describe the thermal plumes generated by radiators and heaters. Musy demonstrated the ability of this class of models to predict temperature fields for various heating or cooling systems.

Finally, Lepers [16] presents good agreement between temperature predictions and measurements in a nonisothermal ventilated room using SAMIRA. The experiment is a full-scale room (7.31 m×2.48 m×2.44 m) designed by Zang et al. [17], in which temperature and horizontal velocity component where meseared with a thermocouple and a hot wire probe, respectively, at 205 locations in the central vertical section. Although velocity predictions are about 2 to 3 times lower than experimental data in the major part of the simulated room, the airflow pattern is qualitatively well represented.

Note that in the zonal methods of the PL-class, what is termed as *pressure* at each cell is a variable internal to the model with no direct physical meaning, certainly with no relationship to the pressure as understood in the building sciences or physics. This prevents matching the pressures in a COMIS-type infiltration airflow model of a complex building, with those of a PL-class zonal model of airflows within a large space enclosed within that building

and in communication with it.

### 3.2 An alternate formulation of zonal models

Axley recently proposed a method to overcome a major shortcoming of the PL class of zonal models [18]. When a PL-class zonal method is applied to model airflow through a room, the total predicted pressure drop across the room depends linearly on the number of cells used. (This shortcoming of the zonal approach has been long known to the practitioners, but no remedy had been proposed for this till now, essentially because the use of zonal models was restricted to single zone buildings where pressure consistency was not an important criterion).

Axley's proposal [18] avoids the grid dependence of pressure in current zonal models. In this approach one assumes that airflow in rooms is determined by the interplay between pressure drops across, and surface drag on, air in each cell. Then the airflow in all cells can be determined by considering the transfer of shear stresses to the nearest wall surfaces. Applying a momentum balance along a differential conduit (see Fig. 2) of height $ds$ and length $\Delta r$ between the pressure node $P_i$ and the pressure node $P_j$, of two adjacent cells leads to:

$$\Delta P_{i,j}\, w\, ds = -\frac{d\bar{\tau}_{sr}}{ds}\, w\, \Delta r\, ds \qquad (2)$$

Using the Prandtl's mixing length expression of shear stress for turbulent flow, and given a velocity profile along the dimension perpendicular to the nearest wall, the cell-to-cell difference of pressure expression becomes:

$$\Delta P_{i,j} \approx 2k_s\, \frac{\kappa^2 a^3 \Delta r}{\rho w^2 \Delta s^3}\, \dot{m}_{i,j}^2 \qquad (3)$$

From now, this model will be called the Surface-Drag model (SD). Like the PL model it can be augmented by adding specific driven flow formulations in specific regions of space. In this latter case, the new SD model with the specific driven flow integrated patch will be called SD-SDF, for Surface-Drag model with Specific Driven Flow.

The next section compares airflow patterns and velocity predictions given by the various formulations of zonal models described above with measurements in a mechanically ventilated isothermal room.

## 4 Comparison with Nielsen's experiment

Nielsen [10] built a rectangular parallelopiped scale model of a room ($H = 89.3\,\mathrm{mm}$) in which the isothermal airflow is expected to be almost two-dimensional (see Fig. 3). The inlet velocity $U_{in}$ is given by the Reynolds number $Re = 5000$ based on inlet slot height ($U_{in} = 15.02\ \mathrm{m{\cdot}s^{-1}}$). Detailed measurements of velocity profiles are provided along four lines through the central vertical plane located at $y = W/2$: two vertical (at $x = H$ and $x = 2H$), and two horizontal (at $z = 0.028H$ and $z = 0.972H$).

We conducted simulations of airflow in the full scale geometry ($H = 3\,\mathrm{m}$) equivalent to Nielsen's experiment, using all four formulations discussed above: PL, PL-SDF, SD, and SD-SDF. In the SDF versions, specific equations describe the jet induced by the inlet slot geometry description of Nielsen's experiment. In these conditions, the inlet velocity is imposed as $U_{in} = 0.447\,\mathrm{m{\cdot}s^{-1}}$. As an alternate simplified method to predict air flows in large spaces, we also applied a coarse-grid conventional $k-\epsilon$ CFD model to this configuration.

Zonal model simulations were performed using the object-oriented simulation environment SPARK, and $k-\epsilon$ CFD simulations were performed with the commercial code StarCD.

In this section, we compare predictions of airflow patterns and velocity profiles using the different models discussed above, as well as the ability of each class of models to predict the total pressure drop across the test room (i.e. across the inlet and the outlet). The pressure drop across the room is directly relevant to the model's suitability for integration with a COMIS-type model for multi-zone airflow in complex buildings.

### 4.1 Airflow patterns

**Power-law model.** For the results presented here, $C = 0.83$ and $n = 0.5$ in equation 1. The results of air flow predictions with the classical (i.e., PL) zonal model are presented in Fig. 4. We see that the predicted air flows are unidirectional (there is no recirculation), and there is no wall jet predicted. The air flow is spread uniformly across the vertical section of the room.

We then added a specific driven flow model to the classical PL model to describe the wall jet downstream of the inlet slot. This jet model is the well-established isothermal wall jet model described by Rajaratnam [19]. The predictions of this PL-SDF model are shown in Fig. 5. The entrainment of

room air into the wall jet is not clearly predicted, nor is recirculation of room air induced by the jet. The jet seems to bounce off the wall opposite the entrance slot and drives a weak recirculation in that region.

**Surface-drag model.** The airflow pattern predicted with the SD formulation (see Fig. 6) is quite similar to the PL model predictions presented in Fig. 4. There is no dominant flow in the room, nor any recirculation induced by the interaction of the jet with the enclosure walls. This SD model is identical to that described by Axley [18], except that Axley used CONTAM [2] to calculate the solution whereas we used the SPARK simulation environment for this purpose. In our implementation we made some improvements over that described in [18]. Mass balance was violated in some cells in the implementation described in [18] (see Fig. 4 of that reference), whereas our implementation satisfies the mass balance everywhere. Detailed results of our implementation are shown in Fig. A.1 which permit comparison with Fig. 4 of [18]. Then we patched the wall jet model developed by Rajaratnam, into this SD Model. The predictions from this SD-SDF formulation are shown in Fig. 7, and are very similar to Fig. 5 for PL-SDF model.

**$k-\epsilon$ CFD model.** We performed air flow simulations in the test case geometry using a conventional $k-\epsilon$ CFD model, using different mesh sizes, ranging from 6×6 to 40×40. Our intention was to characterize predictions from coarse-grid CFD, and compare these with experiment and predictions from various zonal methods. Only for the 40×40 grid did our mesh have grid refinement near wall surfaces to ensure a boundary layer resolution that satisfies the criterion of applicability of wall functions (in this case $y^+<40$). In other, coarser, grids the cell sizes adjacent to the walls were set to 15 cm in the direction perpendicular to the wall.

Chen [20] compared predictions of standard $k-\epsilon$ CFD and his newly developed zero-order turbulence model with Nielsen's experiment. Our 40×40 grid $k-\epsilon$ results agree very well with those of Chen using the standard $k-\epsilon$ model. Fig. 8 shows results for a 10×10 grid, and Fig. 9 shows the 40×40 predictions. Both meshes predict a large recirculation loop due to entrainment in the jet. While slight differences among the four zonal formulations do exist, none predict this recirculation loop, even those for which the specific driven flow model patch predicts the jet itself. The next section presents details of the velocity predictions from the different models, and compares them to experimental data.

### 4.2 Velocity profiles

A comparison of velocity predictions by different zonal models with experimental data along the vertical line at $x = 2H$ is presented in Fig. 10. The air velocities in the wall jet region are well predicted by specific driven flow (PL-SDF and SD-SDF) models (see Fig. 10c), but none of the four zonal model formulations predicts the recirculation. Note that the recirculation is seen as negative velocities below about $z/H = 0.6$ in experimental data plotted in Fig. 10. In addition, results are not significantly different in terms of velocity predictions when comparing SD and PL formulations. Velocity predictions with the four zonal model formulations compare equally poorly with experimental results at other sections of the room: the vertical line at $X = H$, and two horizontal lines, one at $z = 0.972H$ (through the air inlet) and the other at $z = 0.028H$ (through the air outlet). These are not shown for brevity.

The comparison of velocity predictions with coarse grid CFD model is shown for all the four sections of the room mentioned above: the vertical line at $x = H$, and the horizontal lines $z = 0.972H$ (through the air inlet) and $z = 0.028H$ (through the air outlet), in Fig. 11. In this figure, we compare $k-\epsilon$ CFD model predictions for velocities, based on 6×6 and 10×10 grids, to predictions using 40×40 grid and experimental data. Compared to measurements, we see that *all* simulations underestimate the recirculation. The results of the 6×6 and 10×10 grids show a jet decay that is slightly too rapid, but on the whole coarse-grid predictions give satisfactory agreement with the experiment.

These results suggest that coarse-grid conventional $k-\epsilon$ CFD model is a good candidate for simplified predictions of the details of air flows, and consequently of contaminant transport, in large spaces connected to complex buildings. Also, this approach offers a satisfactory agreement with the experimental data in the jet region, even without any expert knowledge to patch a wall jet formula into the computational space at the correct location.

### 4.3 Pressure predictions

Correct prediction of the pressure field is vital for integrating detailed large space model into multizone air flow models. Although the test case we chose has been widely studied, we were unable to find pressure drop data in the literature. In

one case, where researchers had conducted detailed CFD simulations of air flow in this geometry with Large Eddy Simulation, we found that the pressure field files had been discarded because there were thought to be of little interest. Experimentally, it may be impossible to measure pressure drops across the room in this geometry at this flow rate, because the pressure drop is smaller than the detection limit of available research instrumentation.

Zonal (PL and SD formulations) and $k-\epsilon$ CFD models were applied to different grids to predict the total pressure drop between the inlet region and the outlet region of the test room. and the $k-\epsilon$ CFD model. The results are summarized in Fig. 12. As Axley pointed out, the power-law (PL) zonal model predicts a total pressure drop across the test room that is linearly dependent on the number of cells used for dividing the room space. The surface-drag (SD) formulation, as expected, shows no grid dependence. However, it predicts a total pressure drop about 6 times lower than that predicted by the $k-\epsilon$ CFD model for a $40\times40$ grid. This large difference is not entirely unexpected. The SD formulation does not account for molecular and turbulent viscous dissipation of momentum in the core of the room. The coarse-grid CFD results are also sensitive to the number of cells used, although the results appear to flatten asymptotically as the number of cells increases. Thus none of these models qualify for simple coupling to multi-zone air flow models by matching pressures at the connecting surfaces.

Note that in terms of experimental research instrumentation, the lower detection limit for pressure differences is about 0.1 Pa. On the other hand, in Fig. 12, the maximum pressure drop plotted doesn't exceed 0.06 Pa, much below this detection limit. In a real building, interzone pressure differences of the order of 10 Pa are common. Consequently, the pressure drop of 0.01 Pa across the large space can be simply ignored. In that case, the pressure field inside the large space could be kept as only an internal variable inside the large space airflow model, to be used only to support the air flow computation. In the multi-zone air flow model description, the large space would be then considered as a non well-mixed zone represented by a single presure node (with hydrostatically varying pressure). Continuity between both models would be enforced by matching only air flow rates at each aperture that connects the large space to the rest of the building, including the HVAC system components.

# 5 Conclusion

Conventional zonal models were developed to estimate the details of airflow, heat transfer, and contaminant transport rapidly and with sparse input data. This was especially appropriate when computers were slow and expensive. However, the basic formulations (PL and SD) are unable to capture specific driven flows such as wall jets. In case of enhanced models (such as PL-SDF and SD-SDF) with specific patches of idealized driven flows added into the computational space, their accuracy depends essentially on the user's expertise to add appropriate specific driven flow patch models in the correct regions. Other research papers (e.g. Wurtz et al. [11], Lepers [16]), indicate that such models can predict temperature field and low-resolution details of airflows in non-isothermal conditions. The surface-drag formulation yields grid-independent pressure predictions, but ignores the viscous and turbulent momentum dissipation in the core of the flow. Therefore, its prediction of the total pressure drop across the test room is about one order of magnitude below the conventional $k-\epsilon$ CFD model prediction. In addition, the (SDF) reformulation of the zonal model does not improve the poor agreement between the predicted and measured velocity profiles compared to those of the PL and SD formulations, in the regions away from the patched idealized specific driven flow. Velocity predictions from coarse-grid $k-\epsilon$ CFD models are in better agreement with measurements. The pressure drop predictions, however, remain grid dependent at least until about $40\times40$ grids. We note that for these 2D $k-\epsilon$ CFD simulations using $10\times10$ grids, the CPU time required was 3.23 s on a SGI-IRIX workstation (13 times more for the $40\times40$ grid). This does not represent a large computational burden.

The above results show the difficulty of accurately predicting the pressure distribution within a large space with any of the zonal models or with a coarse-grid $k-\epsilon$ CFD model. Therefore, it seems impractical to couple any of these simplified models of airflow in a large space with a multi-zone infiltration model by matching pressures and airflows at all common openings. On the other hand, the pressure drops across the large space are so small that they can be ignored for all practical purposes. Therefore, we propose that the first step to predict integrated details of airflow, heat transfer and contaminant transport in large spaces connected to multi-zone buildings, would be to assume the pressure drop across the room to be negligible. One

should only match air flows across apertures between the building and the large space, and take the pressure variation within the space to be hydrostatic (as done in COMIS or CONTAM). Finally, our results suggest that coarse-grid $k-\epsilon$ CFD can be a satisfactory alternative to zonal methods where more accurate details are required, for predicting air flows and contaminant transport in indoor large spaces connected to a complex multi-zone building. In a separate research effort we are adressing acceptable grid-coarseness for satisfactory approximate results and also for extending this approach to mixed convection configurations.

## Acknowledgements

This research was supported by the Office of Non-proliferation and National Security, Chemical and Biological Non-proliferation Program of the U.S. Department of Energy under Contract No. DE-AC03-76SF00098. We would like to thank particularly Elizabeth Finlayson for her generous advice about using the software StarCD, and Dimitri Curtil for his technical help with using SPARK. We would also like to thank Michael Sohn and David Lorenzetti for improving the clarity of this document by their comments.

## References

[1] Feustel H. E. COMIS - an international multizone air-flow and contaminant transport model. *Energy and Buildings*, 30:3–18, 1999.

[2] Walton G. N. Contam96 user manual. Building and Fire Research Laboratory, National Institute of Standards and Technology, 1997.

[3] Inard C. *Contribution à l'étude du couplage thermique entre un émetteur de chauffage et un local. Etudes expérimentales en chambres climatiques.* PhD thesis, National Institute of Applied Sciences (INSA), 1988.

[4] Bouia H., Dalicieux P. Simplified modeling of air movements inside dwelling room. In *Proceedings of the Building Simulation '91 Conference, published by IBPSA (The International Building Performance Simulation Association)*, pages 106–110, 1991.

[5] Rodriguez E and Caceres I. Draft proposal for a stratification predictive model. Technical report, Comission of European Communities, 1993.

[6] Wurtz E. *Three-dimensional modeling of thermal and airflow transfers in building using an object-oriented simulation environment (in French).* PhD thesis, Ecole Nationale des Ponts et Chaussees, 1995.

[7] Li Y., Delsante A., Symons J. G. and Chen L. Comparison of zonal and CFD modeling of natural ventilation in a thermally stratified building. In *Proceedings of Air Distribution in Rooms Conference (ROOMVENT '98)*, volume 2, pages 415–422, 1998.

[8] Haghighat F., Lin Y. and Megri A. C. Zonal model - a simplified multiflow element model. Technical paper presented at the First International One day Forum on Natural and Hybrid ventilation, HybVent'99, Sydney, Australia, 1999.

[9] Buhl W.F., Erdem A. E., Winkelmann F. C. Recent improvements in SPARK: strong component decomposition, multivalued objects, and graphical interface. In *Proceedings of the Building Simulation '93 Conference, published by IBPSA (The International Building Performance Simulation Association)*, pages 283–289, 1993.

[10] Nielsen P. V., Restivo A. et al. The velocity characteristics of ventilated rooms. *Journal of Fluids Engineering*, 100:291–298, 1978.

[11] Wurtz E., Nataf J.-M. and Winkelmann F. Two- and three-dimensional natural and mixed convection simulation using modular zonal models in buildings. *International Journal of Heat and Mass Transfer*, 42:923–940, 1999.

[12] Voeltzel A. *Dynamic Thermal and Airflow Modeling of Large Highly Glazed Spaces (in French).* PhD thesis, LASH - ENTPE, 1999.

[13] Bouia H. *Modélisation simplifiée d'écoulements de convection mixte interne: Application aux échanges thermo-aérauliques dans les locaux.* PhD thesis, University of Poitiers, 1993.

[14] Musy M. *Automatic generation of zonal models to perform airflow and thermal simulation in buildings (in French).* PhD thesis, LEPTAB - University of La Rochelle, 1999.

[15] Inard C., Bouia H. and Dalacieux P. Prediction of temperature distribution in buildings

with a zonal model. *Energy and Buildings*, 24:125–132, 1996.

[16] Lepers S. *Modélisation des écoulements de l'air dans les bâtiments à l'aide des codes CFD. Contribution à l'élaboration d'un protocole de validation.* PhD thesis, National Institute of Applied Sciences (INSA), 2000.

[17] Zang J. S., Christianson L. L., Wu G. J. and Riskowski G. L. Detailed measurements of room air distribution for evaluating numerical simulation models. *ASHRAE Transactions*, (98)1:58–65, 1992.

[18] Axley J. Zonal models using loop equations and surface drag cell-to-cell flow relations. In *Proceedings of Air Distribution in Rooms Conference (ROOMVENT 2000)*, pages 235–240, 2000.

[19] Rajaratnam N. *Turbulent Jets.* Elsevier Scientific Publishing Company, Amsterdam, 1976.

[20] Chen Q., Weiran X. A zero-equation turbulence model for indoor airflow simulation. *Energy and Buildings*, 28:137–144, 1998.

# Figures

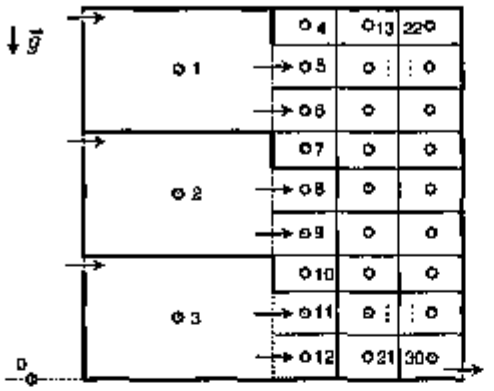


Figure 1: Section of a multizone building

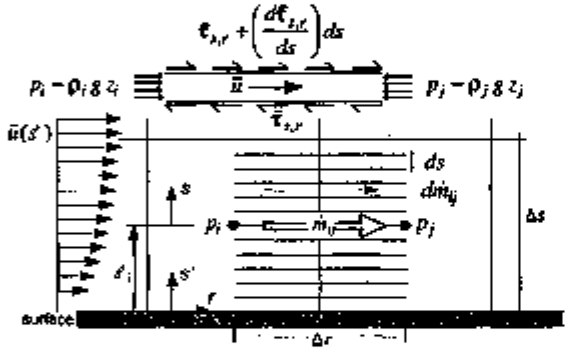


Figure 2: Surface drag momentum balance flow model (figure 2.b in [18])

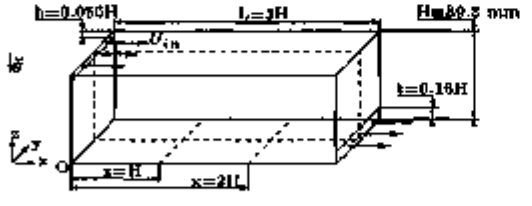


Figure 3: Nielsen's experiment

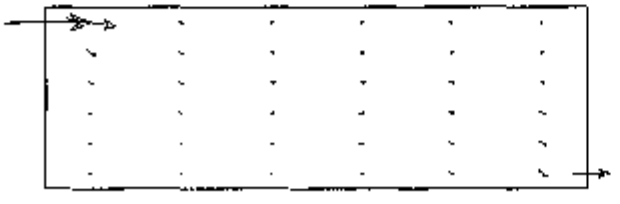

Figure 4: Airflow pattern for the PL model

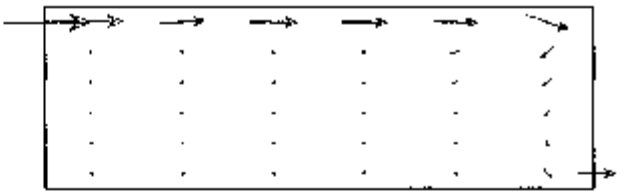

Figure 5: Airflow pattern for the PL-SDF model

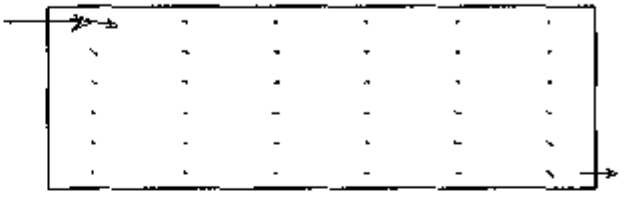

Figure 6: Airflow pattern for the SD model

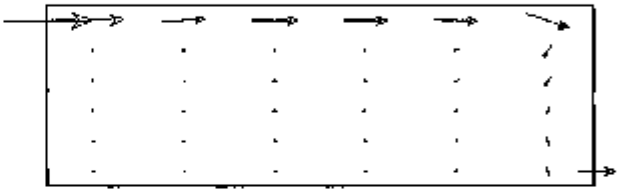

Figure 7: Airflow pattern for the SD-SDF model

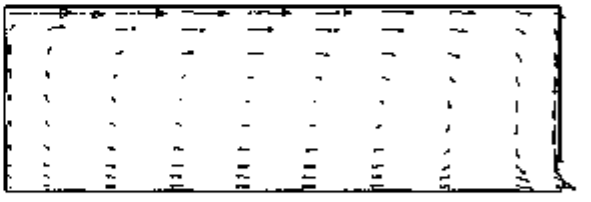

Figure 8: Airflow pattern for the a 10×10 coarse-grid $k-\epsilon$ CFD model

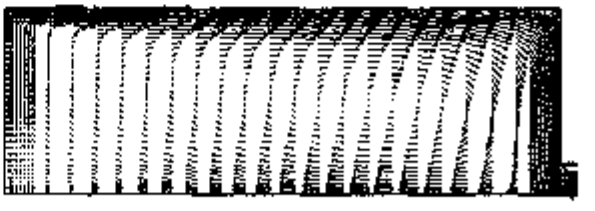

Figure 9: Airflow pattern for the a 40×40 coarse grid $k-\epsilon$ CFD model

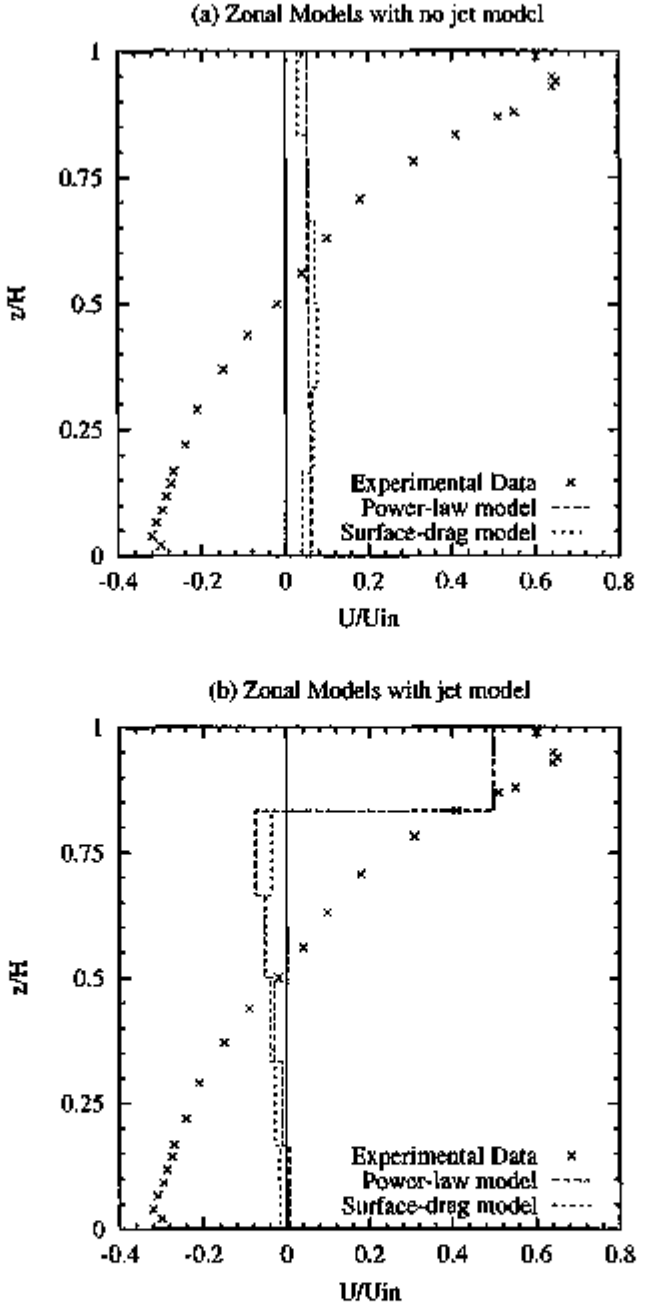


Figure 10: Comparison of velocity profiles predicted by zonal models with experimental data, in the center section at $x = 2H$

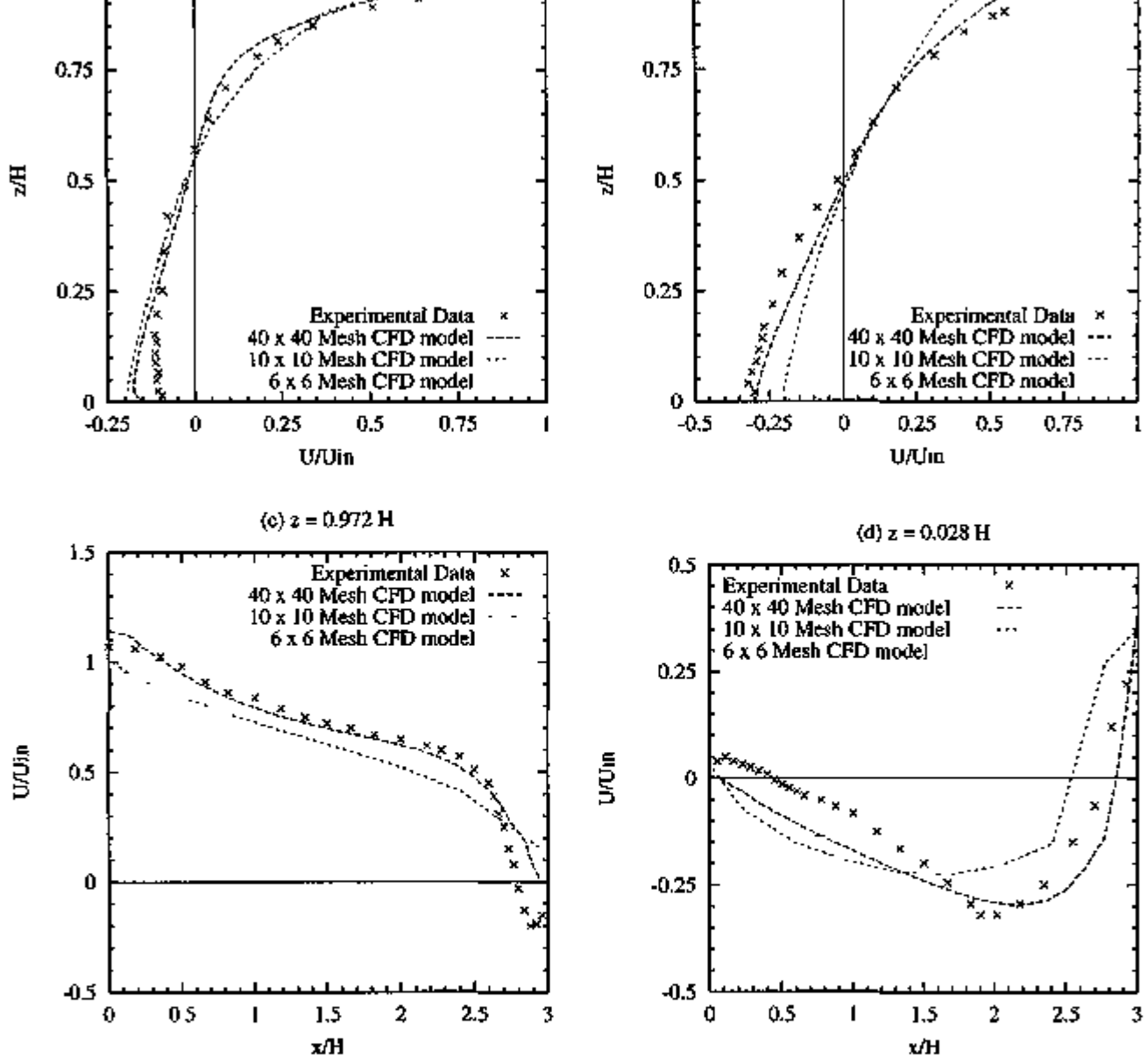


Figure 11: Comparison of velocity profiles predicted by CFD models and experimental data in four sections of the room: (a) at $x = H$, (b) at $x = 2H$, (c) at $z = 0.972H$ and (d) at $z = 0.028H$

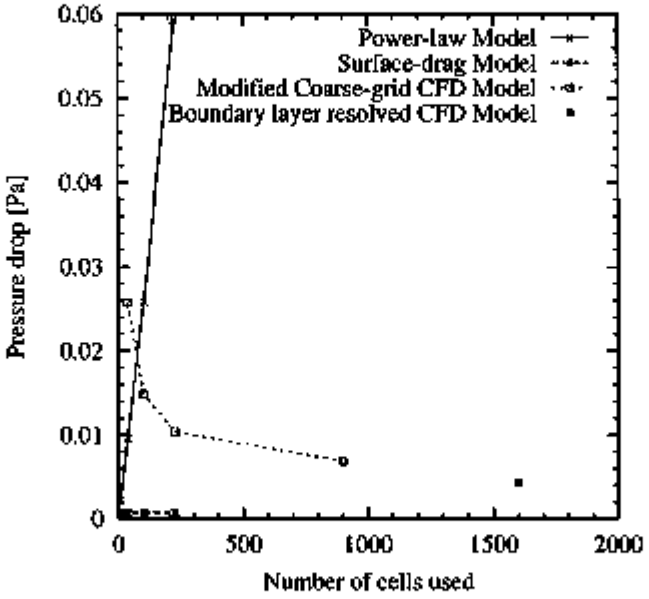


Figure 12: Total pressure drop across the test room

# Appendix

## A Detailed surface-drag model airflow results

Figure A.1 presents mass flow rates obtained when reproducing the simulation of airflow in the Nielson test case. After convergence, the error in mass airflow balance is less than $10^{-4}\,g{\cdot}s^{-1}$ in each cell.

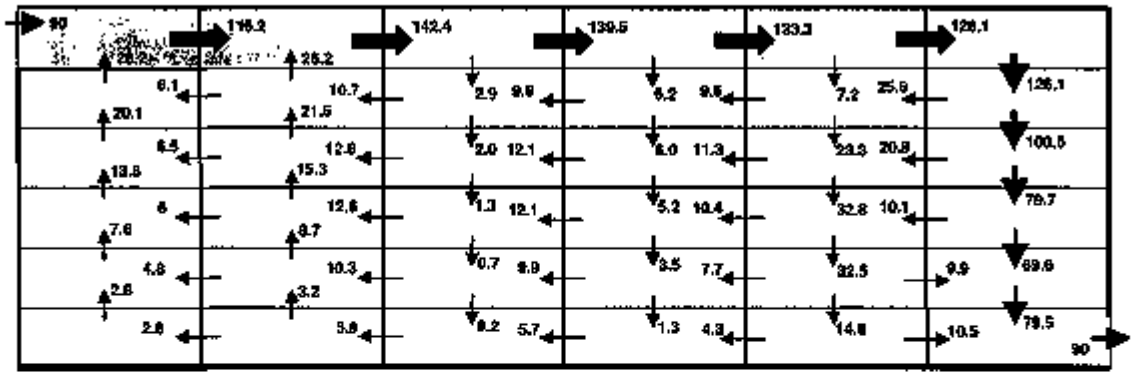


Figure A.1 Mass airflow rates obtained with SD-SDF model (in $g{\cdot}s^{-1}$)